Compensating for attenuation by inverse *Q* filtering

Carlos A. Montaña and Gary F. Margrave

ABSTRACT

Three different approaches for inverse *Q* filtering are reviewed and assessed in terms of effectiveness in correcting amplitude and phase, computational efficiency and numerical instability. The starting point for the three methods is the linear, frequency-independent *Q* theory, in which an attenuated trace can be forward modeled as the product of a wavelet matrix, an attenuation matrix and the earth reflectivity series. In the first method the reflectivity series is solved by inverting a matrix similar to the attenuation matrix with minimized nearly-singular characteristics. The second approach is based on the downward continuation migration method and is a highly efficient and numerically stable method. The last assessed method uses the generalized nonstationary Fourier integrals to apply the inverse *Q* filter. The performance of the three kinds of filters is assessed by assuming that the exact value of *Q* is available. One synthetic trace is created with a pulse source to avoid introducing error by ignoring the conmutator term which is required when the *Q* filter is applied before a spiking deconvolution to remove the source signature. Several attenuated traces are forward modeled for different *Q* values, and used to test the filters. Two attributes are used to quantify the similarity between the expected and the real output: the L2 norm of the difference between the expected and the real output and the maximum crosscorrelation and its corresponding lag, computed for windowed fragments of the traces.

INTRODUCTION

Inverse *Q* filtering is one of the methods used in seismic processing to eliminate from the signal the nonstationary characteristics generated by attenuation processes. Seismic waves traveling through inelastic media are attenuated by the conversion of elastic energy into heat. At being attenuated the traveling wave experiment some distortions: amplitudes are reduced, traveling waveform is changed due to high frequency content absorption, and phase is delayed. Attenuation is usually quantified through the quality factor *Q*: the ratio between the energy stored and lost in each cycle due to inelasticity.

It is generally accepted that the *Q* constant model (Kjartansson, 1979) is a good representation of the attenuation process for most crustal rocks in the range of useful frequencies for seismic processing. Constant *Q* model assumes linearity, i.e. the attenuated signal can be considered as a linear combination of attenuated monochromatic components; linearity is a good assumption as long as the attenuation is not extremely high, (*Q*>10). Experimental measurements of attenuation and its effects on traveling pulses force the inclusion of the dispersion phenomenon, the variation of seismic velocities with frequency, into any acceptable theoretical model. Several dispersion relations have been proposed, e.g. Aki and Richards (2001, p. 170) or Kjartansson (1979), which can be used with comparable results in the different versions of forward and inverse *Q* filtering. The incorporation of causality as a physical constraint on the mathematical models for velocity dispersion, implicitly confers the minimum phase characteristic on the traveling pulse.

It is unreasonable to expect high-quality results from conventional seismic data processing algorithms, designed for stationary signals, when applied to nonstationary signals. Improving the stationary character of the seismic trace is an important step in obtaining the best possible seismic image. When reliable estimations of *Q* are available, for example from VSP data, inverse *Q* filtering is practically the natural method to compensate for the effects of the attenuation process on the seismic signal.

Different methods to apply forward and inverse *Q* filtering can be applied. In the forward *Q* filter, each method is characterized by a particular accuracy and computational speed that makes it more or less practical according to the modeling necessities. In the inverse *Q* filter, besides the accuracy and the computational cost that grows considerably, the numerical stability is an additional critical issue to consider. In this paper three different methods to apply inverse *Q* filter are reviewed and compared: inverting a *Q* matrix or an equivalent *Q* matrix (Hale, 1981); downward continuation inverse *Q* filter (Hargreaves and Calvert, 1991) and (Wang, 2002) and nonstationary inverse *Q* filter (Margrave, 1998).

THEORY

Constant *Q* attenuation model

A simple and powerful model to represent seismic wave propagation in attenuating medium has been developed and broadly accepted in the Geophysicists community. The model is based on the assumptions of linearity, frequency-independent *Q*, and velocity dispersion. In particular, linearity and constant *Q* are approximately valid on the range of useful frequencies in seismic processing. In the context of attenuation, linearity means that the signal can be analyzed into and synthesized from elementary plane waves components on which attenuation can be applied and study independently from each other.

The quality factor *Q* is a parameter used to characterize attenuation in anelastic media. It is defined as the ratio between the energy of the seismic wave and the energy lost in each cycle. The constant *Q* model theory (Kjartansson, 1979) predicts and amplitude loss:

$$A(x) = A_0 \exp\left(\frac{-\omega x}{2 \upsilon Q}\right). \qquad (1)$$

where ω is the angular frequency, υ the velocity, A_0 the initial amplitude and *A(x)* the amplitude at the traveled distance *x*. The experimental measurements on pulses traveling through attenuating media force the inclusion in the model of a frequency dependent velocity. Different velocity functions have been proposed. Aki and Richards (2002) show that the following relation should be held to honor causality,

$$\frac{\omega}{\upsilon(\omega)} = \frac{\omega}{\upsilon_\infty} + \mathrm{H}\left[\frac{\omega}{2\upsilon_\infty Q}\right], \qquad (2)$$

where $\mathrm{H}\left[\dfrac{\omega}{2\upsilon_\infty Q}\right]$ denotes the Hilbert transform of the expression $\dfrac{\omega}{2\upsilon_\infty Q}$ and υ_∞ is the limit of the velocity function when ω tends to infinity. They also show that over the range of frequencies useful in seismic processing an accepted good approximation for the ratio of two velocities at two different seismic frequencies ω_1 and ω_2 is given by

$$\frac{\upsilon(\omega_1)}{\upsilon(\omega_2)} = 1 + \frac{1}{\pi Q}\log\left(\frac{\omega_1}{\omega_2}\right). \qquad (3)$$

Equation (3) is plotted for different Q values in figure 1. Futerman (1962) and Kjartansson (1979) propose alternative velocity dispersion functions, which are different in shape but approximately equal in value for the range of frequencies of common use in seismic processing.
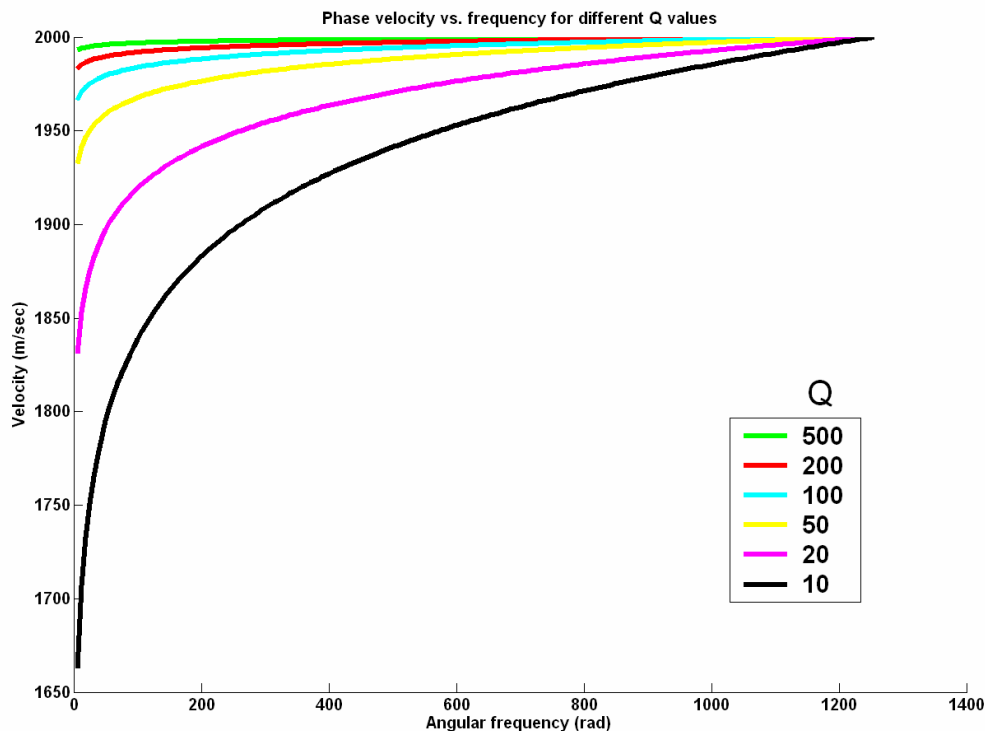

FIG. 1. Phase velocity vs. frequency for different Q values. The curves correspond to the velocity dispersion according to equation (3) using 2000 m/sec as reference velocity at a reference frequency of 400π rad.

The impulse response $b(t)$ is the wavelet that results from a perfect pulse source, or mathematically, a delta function source. In a linear problem it has an enormous importance because the response to any arbitrary source wavelet can be obtained as the

convolution of the source wavelet with the impulse response. Kjartansson (1979) shows that the Fourier transform of the attenuating medium impulse response is

$$B(\omega) = \exp\left[-\frac{\omega x}{2v_\infty Q}\right]\exp\left[\frac{-i\omega x}{v(\omega)}\right]. \tag{4}$$

A source pulse traveling through an inelastic medium, modeled from equation (4), is shown in figure 2. The inverse Fourier transform of equation (4) non-stationary convolved, according to the theory of nonstationary convolution, (Margrave, 1998), with the reflectivity wavelet yields the attenuated seismic trace for an impulsive source (Margrave et al., 2002):

$$s_Q(t) = \frac{1}{2\pi}\int_{-\infty}^{\infty}\int_{-\infty}^{\infty}\alpha_Q(\omega,\tau)r(\tau)e^{i\omega(t-\tau)}d\tau d\omega, \tag{5}$$

where

$$\alpha_Q(\omega,\tau) = \exp(-\omega\tau/2Q + iH(\omega\tau/2Q)), \tag{6}$$

and $\tau = x/v_\infty$. By a stationary convolution of equation (5) with an arbitrary source wavelet $w(t)$, a general nonstationary trace can be generated,

$$\hat{s}(\omega) = \frac{1}{2\pi}\hat{w}(\omega)\int_{-\infty}^{\infty}\alpha_Q(\omega,\tau)r(\tau)e^{i\omega(t-\tau)}d\tau. \tag{7}$$

Equation (7) shows the result of the stationary deconvolution in the Fourier domain. The 'hat' symbol indicates Fourier transform.

A discrete model for an attenuated seismic trace

The model depicted in the previous section corresponds to signal represented as continuous functions. However in practical seismic processing the signal is discrete which has taken to develop a corresponding discrete model for the attenuated seismic trace. The attenuated seismic trace from an impulsive source, equation (5), in its discrete correspondent expression is

$$s_{Qi} = \Delta t\sum_{j=1}^{n}q_{i-j}^{j}r_j, \tag{8}$$

where Δt is the time domain sample rate, n is the number of samples, r is the sampled reflectivity and q is given by the expression

$$q_{i-j}^{j} = \Delta f\sum_{k=1}^{n}\alpha_{Q\,j}^{\,k}e^{\pi i k(i-j)/(n-1)}, \tag{9}$$

where Δf is the frequency domain sample rate and $\alpha_{Q\,j}^{\,k}$ is the discretized attenuation function. Equation (8) has the form of a nonstationary convolution as defined by Margrave (1998) and can be expressed as a matrix multiplication by considering s_Q and r as column vectors and q_{i-j}^{j} as the elements of a convolution matrix,
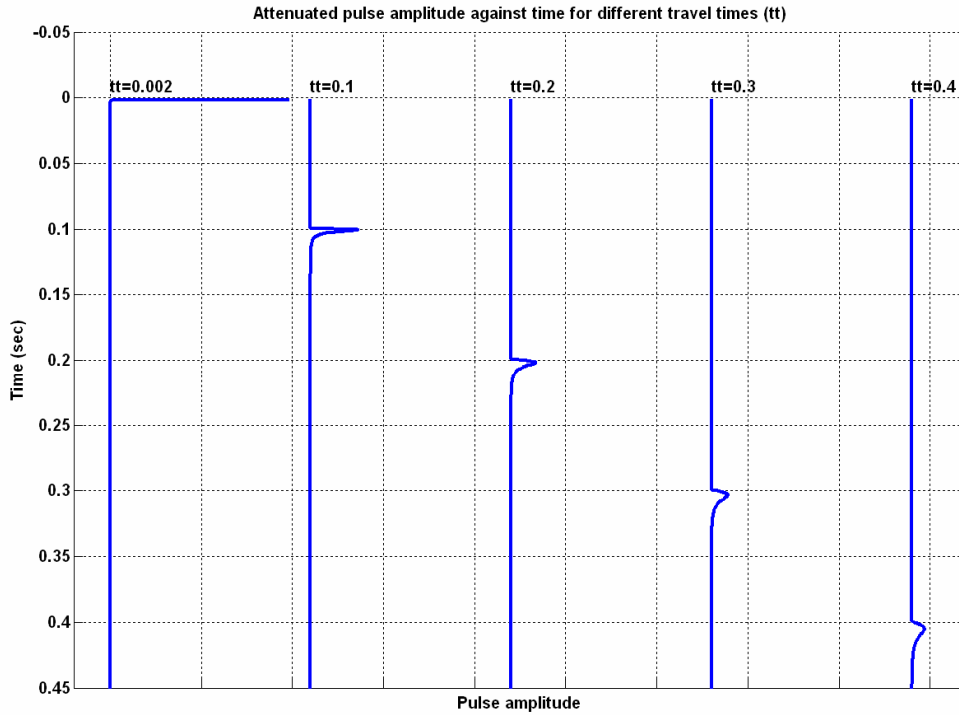
FIG. 2. A pulse traveling through an attenuating medium experiments amplitude decaying, pulse shape change (it gets broader and its decaying time grows faster than its rising time) and growing phase delay. The pulse was modeled using equation (4), for Q=50.

$$s_Q = Qr \,, \tag{10}$$

where Q is the Q matrix which elements are defined by equation (9) and r is the reflectivity vector. The general attenuated trace can be obtained by a discrete stationary convolution between s_Q and an arbitrary source signature, w, which in matrix notation can be written as

$$s = WQr \,, \tag{11}$$

where W is a matrix made up of shifted versions of the source signature as columns as depicted in figure 3.
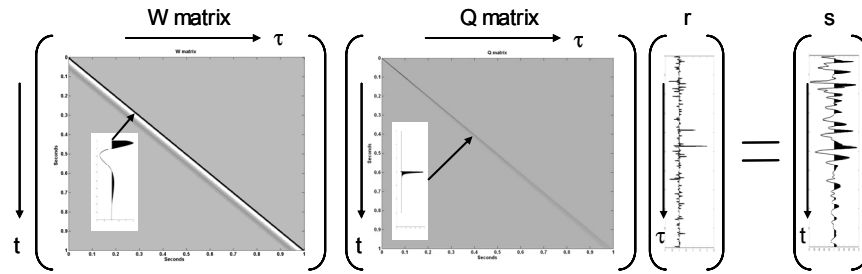
FIG. 3. Graphical representation of equation (11). The attenuated signal *s* can be modeled as the product between the source wavelet matrix, *W*, and the matrix made up of impulse responses at different traveltimes as columns, *Q*, multiplied by the reflectivity vector.

The inverse problem

The objective of processing is to find the reflectivity vector *r* knowing the recorded attenuated signal *s*. This goal could be achieved easily, if the *W* and *Q* matrices were known, by inverting the matrices to obtain

$$r = Q^{-1}W^{-1}s. \tag{12}$$

This last equation indicates that the inverse *Q* filter must be applied after the source signature has been removed from the trace. In practice *W* is unknown, and most of the times can be just estimated with an uncertainty so high that remains useless for practical applications. As a result in practice, to solve for *r* from equation (12), Q^{-1} has to be applied before the source signature estimation and removal, which introduces an error equal to the conmutator between Q^{-1} and W^{-1},

$$\left[Q^{-1}, W^{-1}\right] = Q^{-1}W^{-1} - W^{-1}Q^{-1}. \tag{13}$$

The inverted reflectivity can be expressed with the help of this conmutator as

$$r = W^{-1}Q^{-1}s + \left[Q^{-1}, W^{-1}\right]s. \tag{14}$$

The conmutator is zero just if *W* is an identity matrix, i.e. the wavelet is a perfect pulse (or a delta function). In any other case, by applying an inverse *Q* filter before a spiking deconvolution to remove the source signature, an error is introduced which depends on how different be the source signature from a perfect pulse.

INVERSE Q FILTER METHODS

Inverting the *Q* matrix

The most elementary way to apply an inverse *Q* filter is by building and then inverting a *Q* matrix. Two shortcomings arise when this method is applied: inefficiency and instability. The computational cost of inverting a matrix is estimated as n^3, where *n* is the matrix dimension. The *Q* matrix becomes nearly singular for *Q* values below 70 introducing numerical instability in its inverse estimation.

Hale (1981) proposes a method to build an equivalent *Q* matrix, Q_e, and then inverting it. The Q_e matrix is generated by pre and post multiplying the *Q* matrix by an auxiliary

matrix *P,* whose columns are the inverse of the *Q* matrix columns (inverse in the sense that the convolution between the two columns is a delta function). The inverted trace is thus computed as

$$r \approx W^{-1}(PQ)^{-1}Ps \,. \tag{15}$$

This procedure is as accurate as inverting the *Q* matrix itself and stable for *Q* values above 40, though computationally quite more expensive. The sign $\approx$ is used in equation (15) because the term $[W^{-1},(PQ)^{-1}P]s$ has been thrown away.

The efficiency of Hale's method can be improved by implementing a fast algorithm to create the *Q* and *P* matrices. The first columns of both matrices are spikes. The second column of the *Q* matrix is found by the Kjartansson method, i.e. Fourier inverting equation (4) for $x = \upsilon \Delta t$, where Δt is the sample trace and υ is a test velocity. The second column of the *P* matrix is found by inverting the second column of the *Q* matrix. For j greater than 2, the *jth* column of either matrix is generated by *j-2* self-convolutions of its second column. Though by using this algorithm the computational cost of building the *P* and *Q* matrices is reduced substantially, the total cost is still very high due to the two matrix multiplications, and the matrix inversion that are needed.

Invert *Q* filter by downward continuation

This method is based on a wave propagation approach in which deconvolution and inverse *Q* filtering are processes closely related to inverse wave propagation or migration. Hargreaves and Calvert (1991) incorporate attenuation and dispersion effects into the downward continuation operator of the Gazdag (1978) phase shift method. This technique aims for phase compensation based on the 1D (2-way propagation) wave equation

$$\frac{\partial^2 U(z,\omega)}{\partial z^2} + k^2 U(z,\omega) = 0 \,, \tag{16}$$

where *z* is the depth, *U* is the plane wave of frequency ω and *k* is the wavenumber. In the phase shift migration method the backward propagation process is described by the solution

$$U(z + \Delta z,\omega) = U(z,\omega)e^{ik\Delta z} \quad . \tag{17}$$

The distance increment Δz can be expressed in terms of the phase velocity $\upsilon(\omega_0)$ at the reference frequency ω_0 and the time increment Δt as

$$\Delta z = \upsilon(\omega_0)\Delta t \,. \tag{18}$$

Anelastic attenuation can be included in the wave motion by making the wavenumber complex while keeping the frequency real. In terms of *Q* and the frequency-dependent phase velocity $\upsilon(\omega_0)$, the complex wavenumber is

$$k = \frac{\omega}{\upsilon(\omega)}\left(1 - \frac{i}{2Q}\right). \tag{19}$$

As a seismic trace is the record of the propagation path from the source to the reflector and back to the surface, Hargreaves and Calvert (1991) point out that if Q is constant with position, then the inverse filtering depends only on traveltime and is independent of wave direction. Given this circumstance there is no distinction between prestack and poststack inverse filtering and the separation of the two processes, that is migration and inverse filtering, is exact.

By substituting equation (18) and (19) into equation (17) the following inverse filter is obtained

$$U(t + \Delta t, \omega) = U(t, \omega)\exp\left(\frac{i\omega\upsilon(\omega_0)}{\upsilon(\omega)}\Delta t\right)\exp\left(\frac{\omega\upsilon(\omega_0)}{2Q\upsilon(\omega)}\Delta t\right). \tag{20}$$
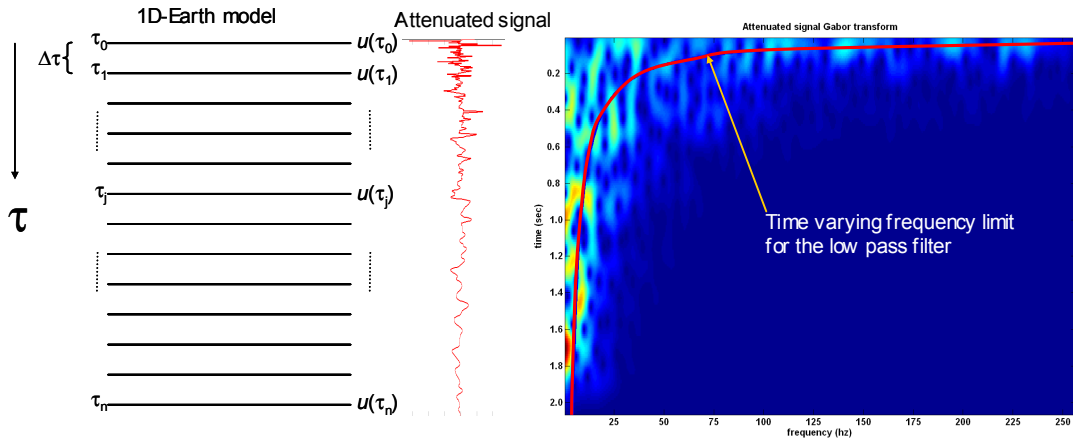

FIG. 4. In inverse Q filter by downward continuation, a 1-D wave equation is used to propagate the wavefield in a migration-like process. A 1-D layered earth model is considered where the field is propagated from one layer down to the next using the downward continuation operator of equation (20). An attenuated trace and its Gabor transformed are shown. To eliminate the instability generated by the real exponent of the operator, Wang (2001) uses a time-varying low pass filter which upper frequency limit is depicted on the Gabor transform.

The first exponential in equation (20) compensates for the phase error introduced by velocity dispersion and the second one for the amplitude decay due to energy absorption that occurs in anelastic attenuation. A velocity dispersion relation such as equation (3) can be used to define $\upsilon(\omega)$ in equation (20).

Downward continuation is applied to each monochromatic component of the signal according to equation (20). The signal in the time domain is found by adding up the elementary plane waves,

$$U(t + \Delta t) = \frac{1}{2\pi} \int U(t + \Delta t, \omega) d\omega . \tag{21}$$

Hargreaves and Calvert (1991) implement a solely phase compensation filter by ignoring the second exponent in equation (20) which causes numerical instability for high values of t/Q. Wang (2001) tackles the stability problem introduced by the second exponent in the filter by limiting the frequencies contributing to the compensation to

$$\omega_q \leq \frac{2Q}{t} . \tag{22}$$

The frequency function in equation (22) determines the upper limit of a time-varying filter; it is plotted over the Gabor transform of the attenuated signal in figure 4 (left). Equations (20) and (21) have to be applied alternatively for each interval Δt to get the filtered signal. Wang (2001) also introduces an efficient layered implementation of the method by averaging the second exponent in equation (20) over the time, the frequency or both domains.

Nonstationary inverse *Q* filter

By definition, convolution is a mathematical operation between stationary signals. A linear filter is characterized entirely by its impulse response, its response to any other input is found by convolving the impulse response with the input which is called the convolutional method.

$$g(t) = \int_{-\infty}^{\infty} a(t - \tau)h(\tau)d\tau . \tag{23}$$

In the convolution integral, equation (23), $g(t)$ is the output $a(t-\tau)$ is the time–delayed filter impulse response, $h(\tau)$ is the input and τ is a shifting time variable.

Margrave (1998) extends the convolutional method to nonstationary filters. This extension results in the introduction of two new operations: nonstationary convolution, equation (24) and nonstationary combination, equation (25),

$$s(t) = \int_{-\infty}^{\infty} b(t - \tau, \tau)h(\tau)d\tau , \tag{24}$$

$$\tilde{s}(t) = \int_{-\infty}^{\infty} b(t - \tau, t)h(\tau)d\tau , \tag{25}$$

where, as in the stationary case, τ is a shifting time variable, $h(\tau)$ is the input signal and $b(t-\tau, \tau)$ or $b(t-\tau, t)$ is the impulse response function in the time domain.

This couple of operations has an equivalent formulation in the frequency domain, equation (26) and (27), which corresponds to the convolution theorem for stationary signals,

$$S(\omega) = \int_{-\infty}^{\infty} B(\omega - \Omega, \Omega)H(\Omega)d\Omega, \tag{26}$$

$$\widetilde{S}(\omega) = \int_{-\infty}^{\infty} B(\omega - \Omega, \omega)H(\omega)d\omega. \tag{27}$$

$\widetilde{S}(\omega)$, $S(\omega)$ and $H(\omega)$ are the 1-D Fourier transform of *s(t)*, $\widetilde{s}(t)$ and *h(t)* respectively and $B(\omega - \Omega, \omega)$ is the 2-D Fourier transform of the impulse response function $b(t - \tau, t)$.

The theory is extended by expressing the two new operations, nonstationary convolution and combination, in mixed time-frequency domains which turn out to be generalized Fourier integrals. Nonstationary convolution on the mixed time-frequency domain results a generalized forward Fourier integral and is expressed by the relation

$$S(\omega) = \int_{-\infty}^{\infty} \beta(\omega, \tau)h(\tau)e^{-i\omega\tau}d\tau, \tag{28}$$

where $\beta(\omega, \tau)$, the nonstationary transfer function, is the 1-D Fourier transform of the impulse response function $b(t - \tau, \tau)$ with respect to the variable $t - \tau$. In an analogous way nonstationary combination in the mixed time-frequency domain is a generalized inverse Fourier integral and is expressed as

$$\widetilde{s}(t) = \frac{1}{2\pi} \int_{-\infty}^{\infty} \beta(\Omega, t)H(\Omega)e^{i\Omega t}d\Omega. \tag{29}$$

Equations (28) and (29) may be used to apply nonstationary filtering and specially as efficient and stable ways for forward and inverse *Q* filtering. In the forward case the nonstationary transfer function is equal to $\alpha(\omega, t)$ as defined in equation (6). For the corresponding inverse *Q* filter the nonstationary transfer function is the arithmetic inverse function $\alpha(\omega, t)^{-1}$.

Examples

To test the performance of the three methods of inverse *Q* filtering, a synthetic random reflectivity series was created. This reflectivity series is used as reference trace, without convolving it with any source wavelet, which is equivalent to have a pulse source, avoiding in this way to deal with the error introduced by ignoring the conmutator term in equation (14) when applying inverse *Q* filtering. A forward *Q* filter was applied to the reference trace, for different *Q* values, using the Kjartansson method, i.e. multiplying the reference trace by a *Q* matrix, whose columns are created by Fourier inverting equation (4) and then applying a time shifting. The original and modeled attenuated signals are shown in figure 5.
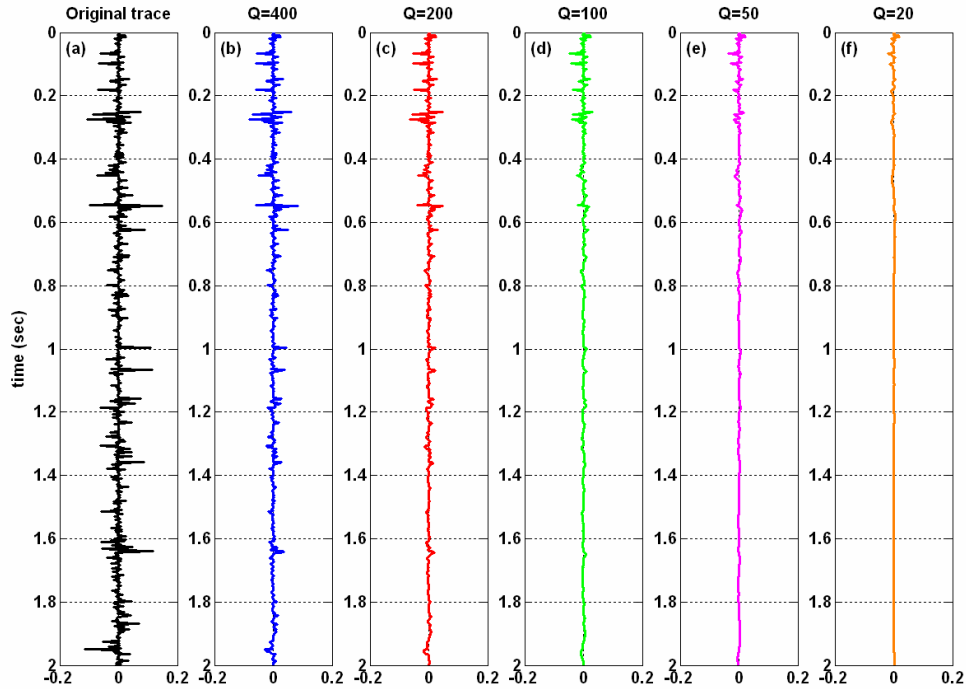
FIG. 5. Original synthetic random reflectivity series (leftmost) used as reference stationary trace to generate the attenuated traces shown to its right, by applying a forward filter with a constant *Q* value indicated at the top of each trace.

The performance of the different inverse *Q* filter methods is evaluated by estimating the error generated by the filtering process. A first attribute to estimate the error is generated by taking the Gabor transforms of the non attenuated reference signal and the inverse *Q* filtered signal, resting one from the other and finally computing the L2 norm for each time row of the transforms difference. For this attribute a perfect match between both traces would generate a value of zero for the error. As the traces differentiate more and more one from the other, the error grows without an upper limit.

A second attribute is obtained by crosscorrelating the reference trace and the inverse *Q* filtered trace; the maximum crosscorrelation gives a measure of how similar are the two traces and the lag at which the maximum crosscorrrelation occurs can be interpreted as an estimation of the remaining error in the phase. This attribute has a global meaning but a local estimation of the similarity between the traces can be obtained by crosscorrelating short fragments of the traces as shown in figure 6. The maximum crosscorrelation coefficient varies from 0 for total dissimilarity, for two different random series absolutely uncorrelated, to 1, for two identical signals.
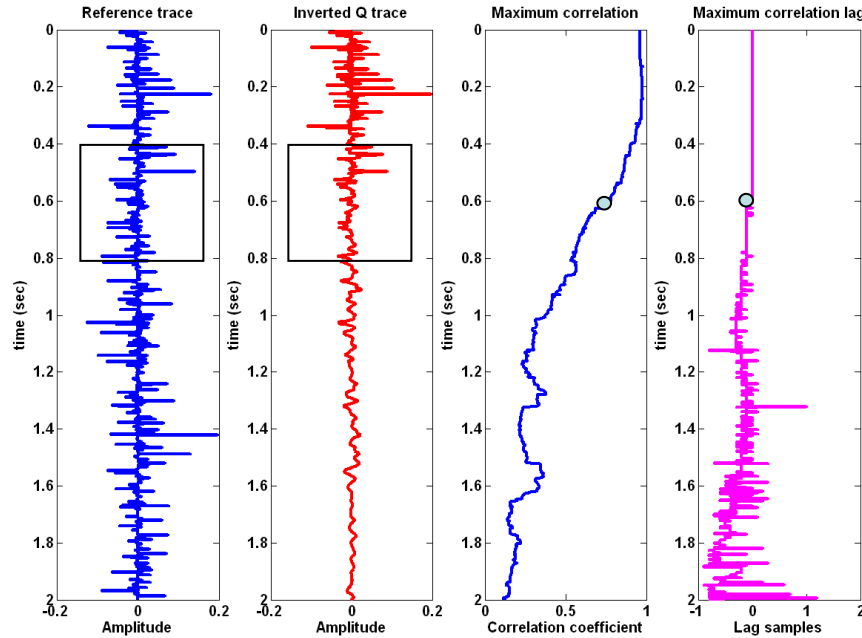
FIG. 6. To use crosscorrelation as a local indicator of similarity between two traces, the crosscorrelation between two fragments is computed. The maximum coefficient and its lag are taken as attributes (two rightmost panels) for the midpoint of the time window. The window is time shifted one sample to find the attributes for the following point.

Figure 7 shows the results obtained by applying Hale inverse Q filter to the attenuated traces. The original reference trace is recovered perfectly for Q values equal or greater than 50 as can be observed by simple visual inspection or by assessing their similarity attributes shown in figure 7 (**g**), (**h**) and (**i**). The L2 norm is nearly zero; the maximum crosscorrelation is virtually one at a lag of zero samples, all of which indicates that the two traces are practically identical. For Q values lesser than 40, the matrix inversion solution starts to blow up, for example for Q=20, the signal piece between approximately 0.22 and 0.9 seconds is totally distorted. However the other pieces of the signal have been almost perfectly restored.

Figure 8 shows the results obtained by applying downward continuation inverse Q filter to the attenuated traces shown in figure 5. A progressive deterioration of the quality solution is observed when Q decreases. Also, along each trace a deterioration of the solution can be observed when time increases. These observations are quantitatively expressed in the corresponding similarity attributes of figure 8 (**g**), (**h**) and (**i**). It is interesting than the maximum crosscorrelation lag for Q equal or greater than 50 keeps below one sample, which can be interpreted as a very good phase correction.
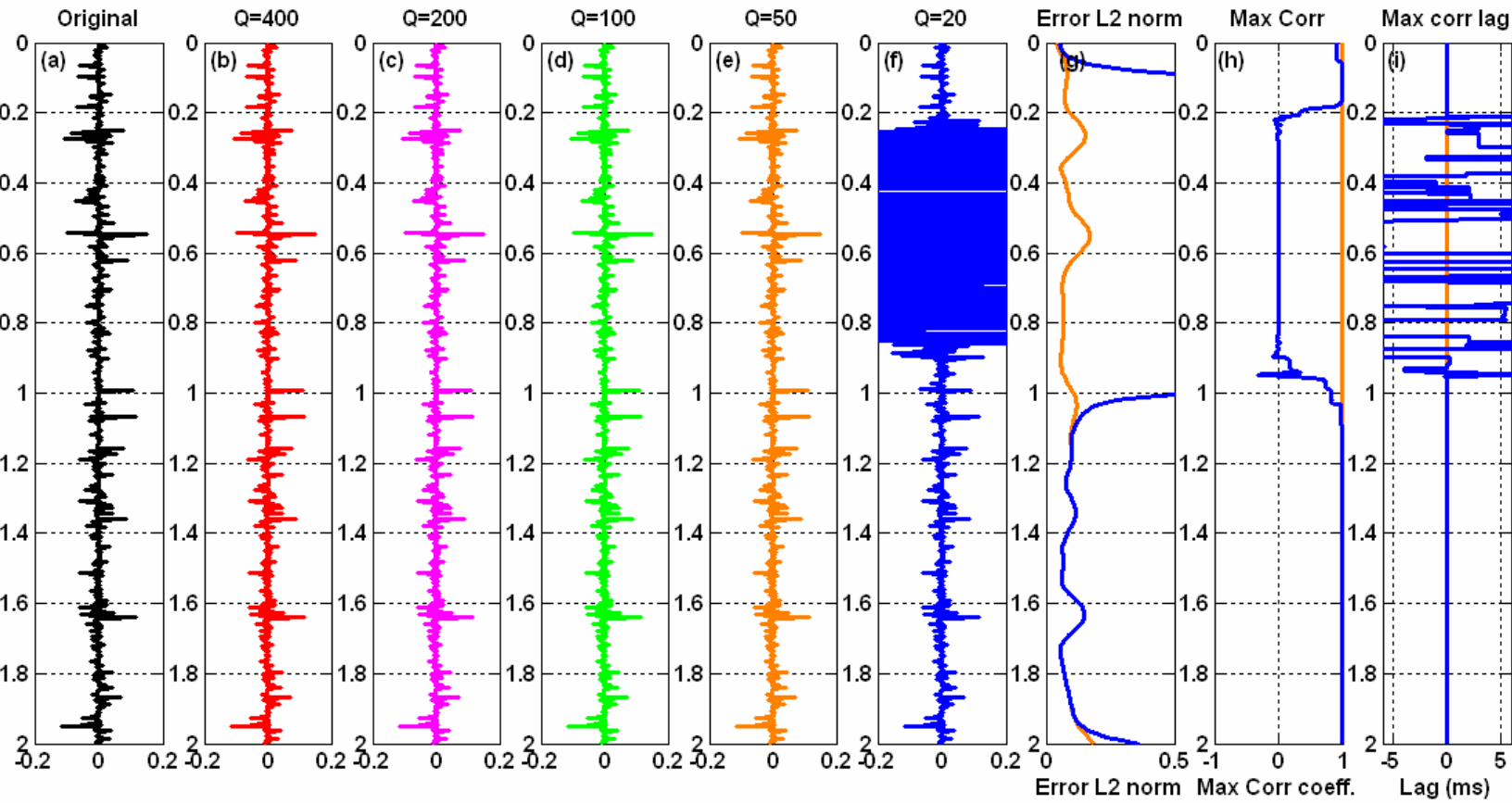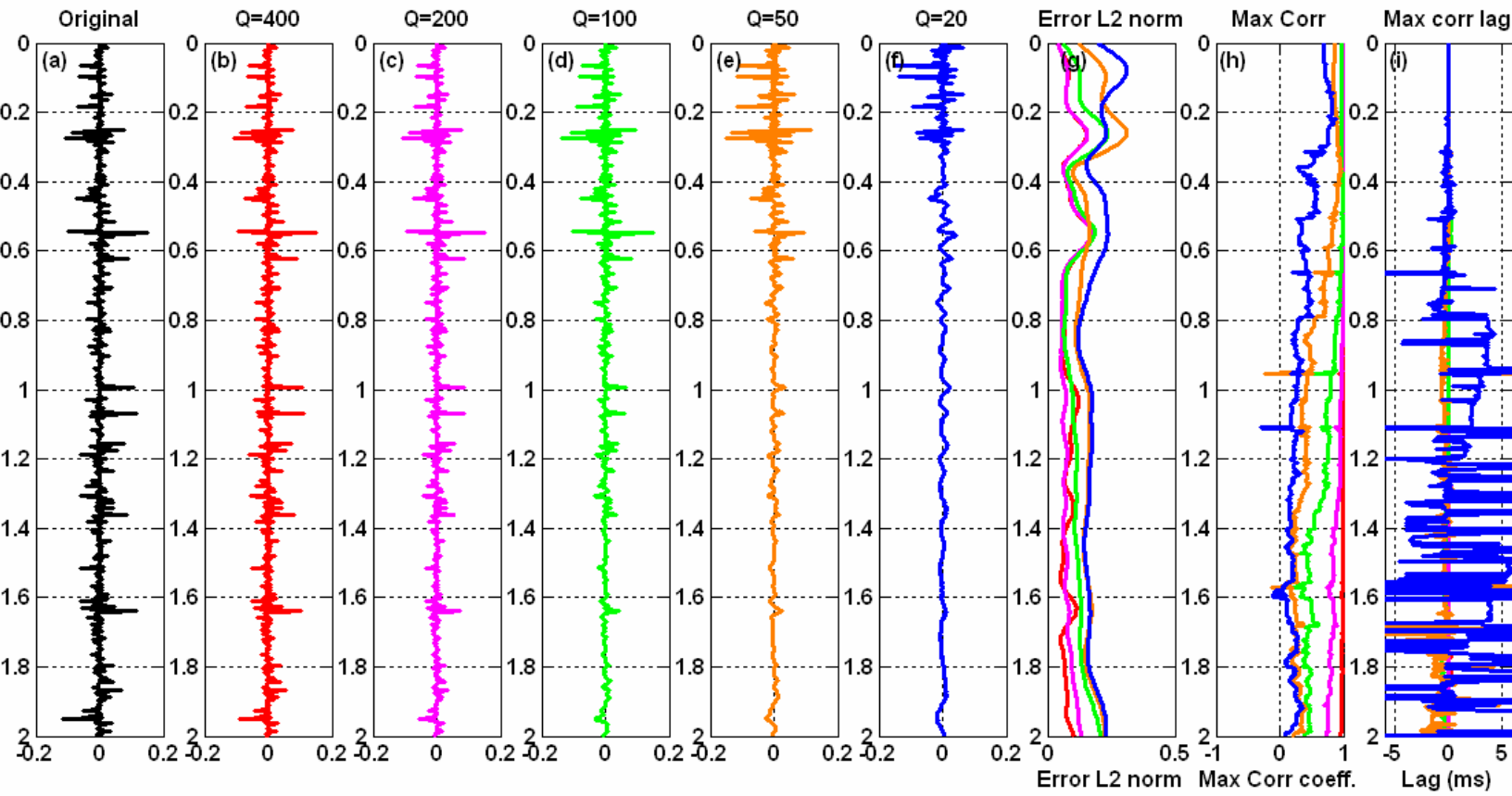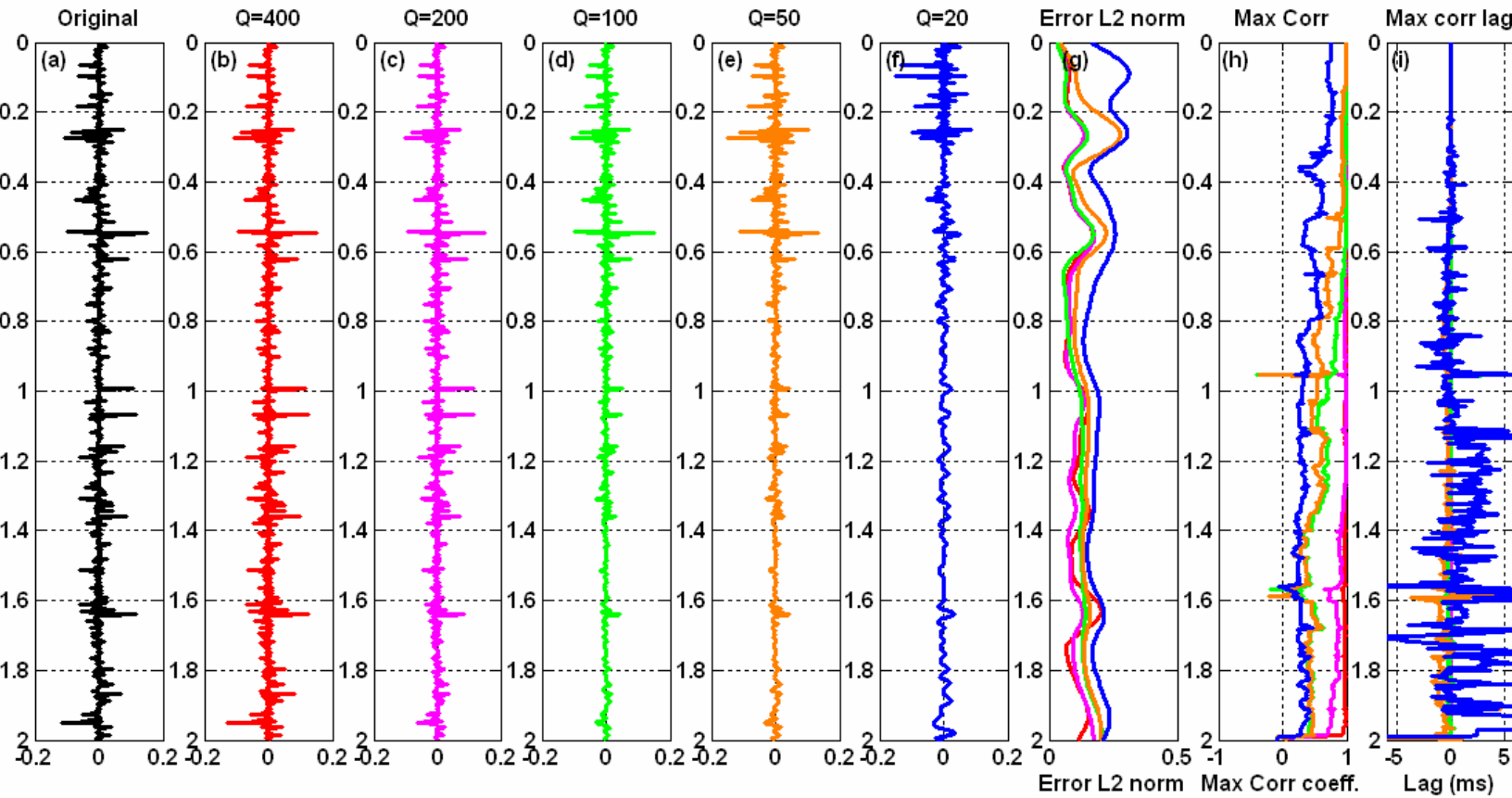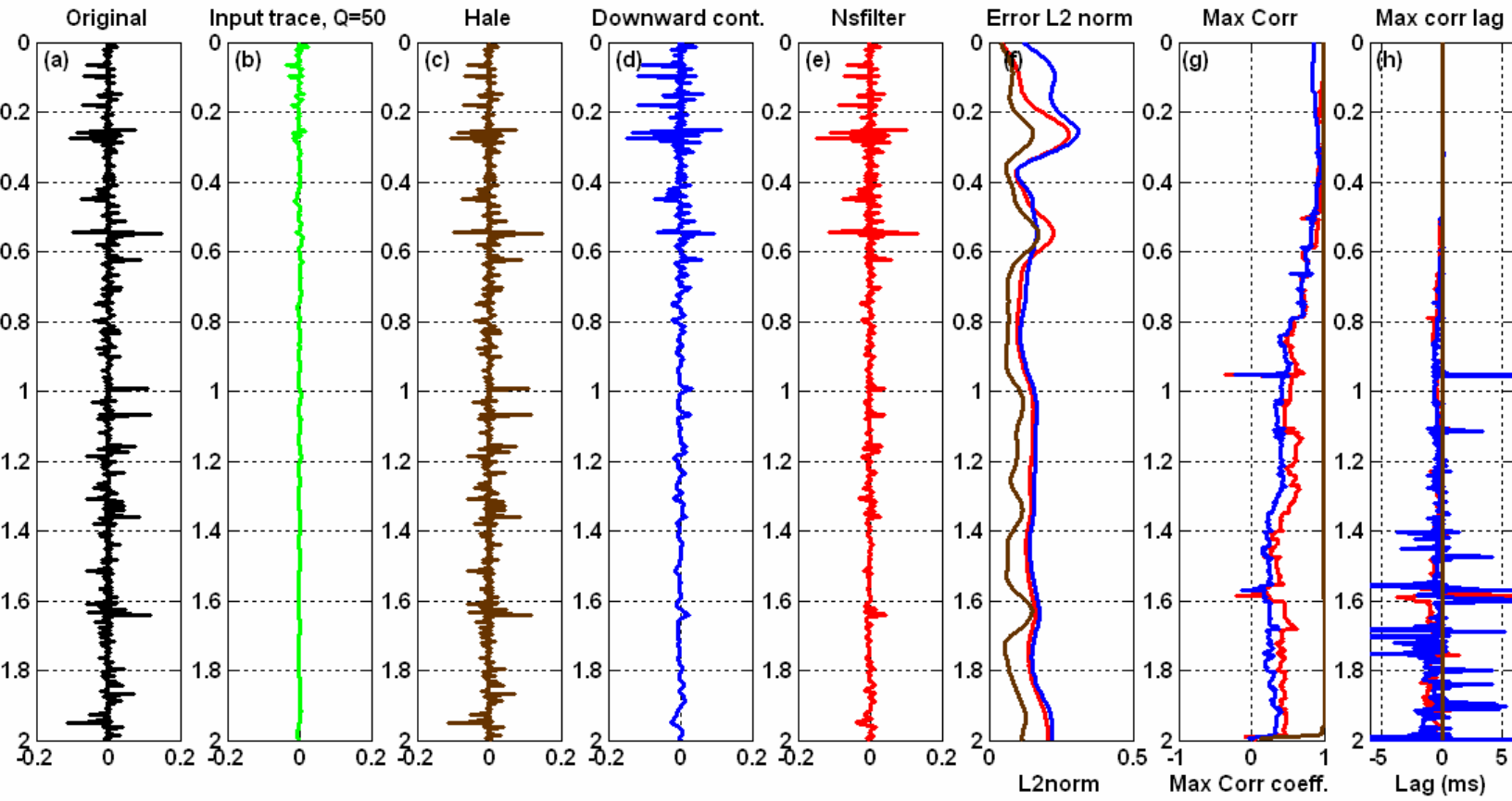
7. The traces in figure 5 after inverse *Q* filtering using the Hale's matrix inversion method. The original trace (**a**) is shown again as refere... ...esults are almost perfect, except for *Q*=20 where the fragment between 0.22 and 0.9 seconds has not been solved at all. Along the wh... ... for *Q* equal or greater than 50, (**b**) (**c**) (**d**) and (**e**), the L2 norm error (**g**) is very small, the maximum crosscorrelation coefficient (**h**) is one ... (**i**) zero. Just for the piece of (**f**), corresponding to Q=20, this method could not get a solution. This kind of stability is present for Q va... ... than approximately 40.

FIG. The traces in figure 5 after inverse *Q* filtering using the downward continuation method. The original trace (**a**) is shown again as reference. ng inability to recover amplitudes, when *Q* decreases and/or time increases, can be observed. The phase correction (**j**) is very good excep. The amplitude correction (**g**) and (**h**) decays in quality when Q decreases.

9. The traces in figure 5 after inverse *Q* filtering using the nonstationary inverse *Q* filter method. The original trace (**a**) is shown again ... nce. . A growing inability to recover amplitudes, when *Q* decreases and/or time increases, can be observed in (**g**) and (**h**), though the res... etter than in the downward continuation case. The phase correction (**j**) is very good except for Q=20.

10. Comparison of the three methods for *Q*=50. The reference trace (**a**), expected output, and the attenuated trace (**b**), input, are show
nces. (**c**), (**d**) and (**e**), real outputs, show the results after filtering the attenuated trace by applying the different methods for inverse *Q* filter
est results are for Hale's method (**c**). Events in the nonstationary filtered trace (e) are easier to resolve than in the downward continua
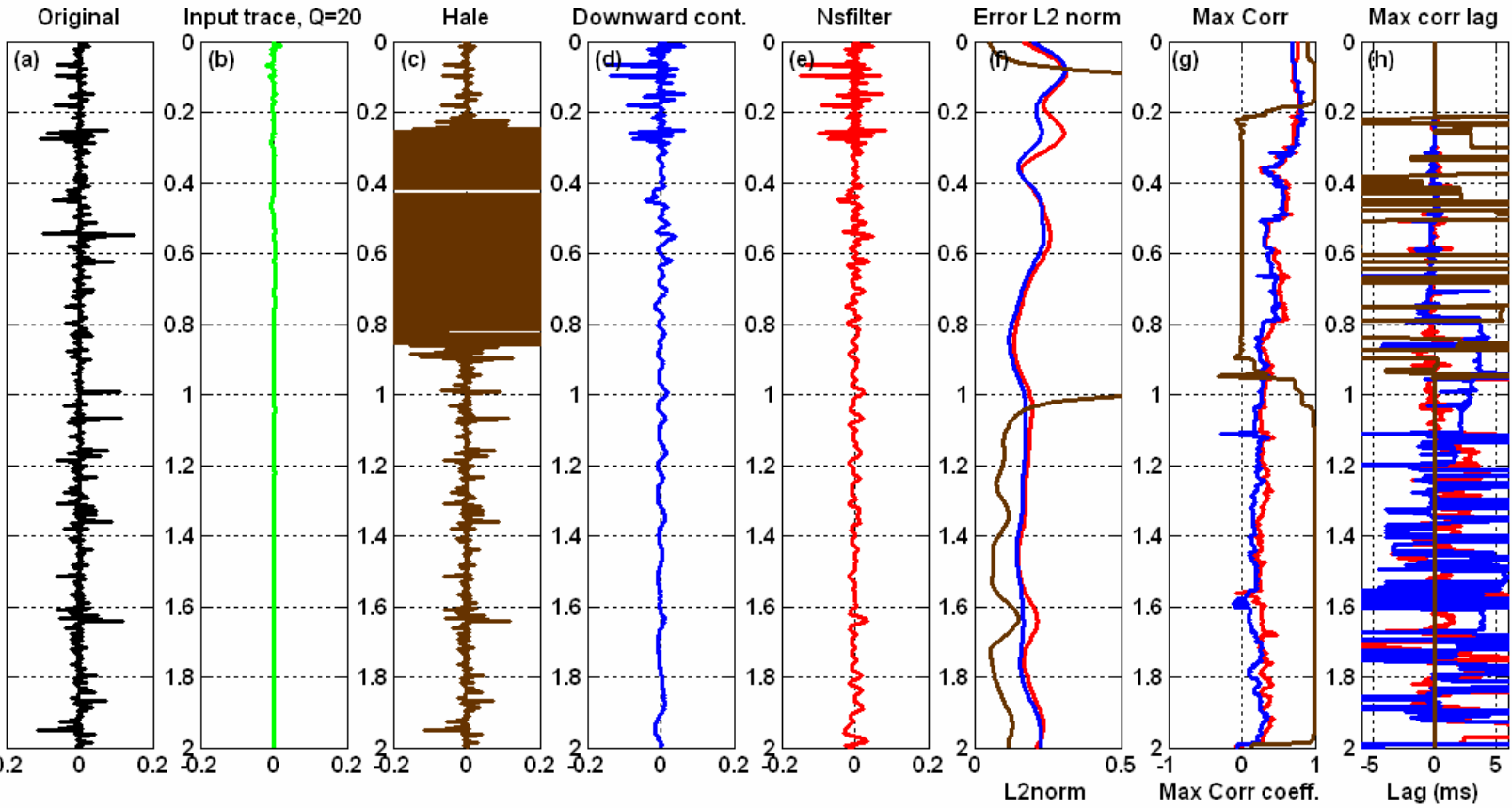d trace (**e**).

1. Comparison of the three methods for *Q*=20. The reference trace (**a**), expected output, and the attenuated trace (**b**), input, are shown...nces. (**c**), (**d**) and (**e**), real outputs, show the results after filtering the attenuated trace by applying the different methods for inverse *Q* filter...best results are for Hale's method (**c**). Events in the nonstationary filtered trace (e) are much easier to resolve than in the downw...uation filtered trace (**e**).

Figure 9 shows the results obtained by applying nonstationary inverse Q filter to the attenuated traces shown in figure 5. A progressive deterioration of the quality solution is observed when Q decreases and/or time increases similarly to the perceived for the downward continuation case. The tendencies and values of the corresponding similarity indicators of figure 9 (**g**), (**h**) and (**i**), are also similar to the ones found for the downward continuation case, though in this case the crosscorrelation is much better.

A direct comparison of the performance of the three methods is shown in figure 10 for Q=50 and figure 11 for Q=20. In this direct comparison, big differences in favor of the nonstationary inverse Q filter compared to the downward continuation method are observed. Hale's method keep being the best when instability does not show up.

DISCUSSION

Inverse Q filter methods can be used when reasonable estimations of Q are available. However a high degree of uncertainty accompanies any practical estimation of Q. Many factors contribute to the uncertainty associated with attenuation measurements Depending on the method used, very different values of Q can be obtained (e.g. Solano and Schmidt, 2004). The uncertainty increases if the variation of Q with depth is considered.

However in the examples shown in this paper the incidence of uncertainty accompanying any estimation of Q is not taken into consideration. This issue is considered in Montana and Margrave (2004). In this work the three methods to apply inverse Q filter are tested under the assumption that Q is known with 100% of certainty.

The main characteristics to assess in each method are effectiveness, efficiency and stability. With respect to effectiveness for Q values greater than 40, Hale's matrix inversion is the absolute winner, with practically 100% of accuracy both in amplitude and phase restoration. Additionally is remarkable that the pieces of trace solved for Q=20, are also almost perfectly restored. The performance of the other two methods at this respect is poor in amplitude restoration and acceptable in phase correction, if it is accepted that the maximum crosscorrelation lag is a reliable estimation of the remaining phase error after the filter is applied. In contrast to the other methods which increase their powerlessness with depth, Hale's method start to blow up in an intermediate zone of the signal. Different algorithms for inverting matrices, available in MATLAB, were used without reaching better results that the ones shown in figure 7.

Considering efficiency, Hale's method is the absolute looser, its computational speed is around $O(n^4)$ where n is the samples in the trace. This elevated cost is caused by the necessity of 4 matrix multiplications, a matrix inversion, and as many as $2n^2$ convolutions (or 2n FFTs) to ensemble the Q and P matrices. This is a really high cost which can be paid if the same filter can be used for a gather of traces and if there is no need of an iterative process in which at each step a different filter has to be used, as in an optimization process. Downward continuation computational speed is $O(n^2\log(n))$, consequence basically of n FFTs. This cost is reduced when the layered version of the algorithm is applied, where the field is propagated directly from the top to the bottom of the layer and the field in between is computed by interpolating the real exponential in the

operator. The nonstationary inverse Q filter has an intermediate efficiency that can be improved by using nonstationary combination and interpolating in the frequency domain.

Downward continuation and nonstationary inverse Q filtering approaches are highly stable for the range of Q values where the attenuation can be considered linear, i.e. Q greater than 10. In addition to efficiency, the other flaw for the Hale's matrix inversion method is the arising of numerical stability problems for Q values below 40. Moreover the algorithm gets unstable for higher values when the used Q does not correspond to its exact value.

CONCLUSIONS

Three different methods to apply inverse Q filter has been reviewed, evaluated and compared, under the assumption that an exact estimation of Q is available. The Hale's matrix inversion approach produces a filtered trace practically identical to the expected output for Q values greater than 40. The shortcomings of this method are its elevated computational cost and its instability for Q values lesser than 40. A second approach to inverse Q filtering assessed is a downward continuation implementation. This is the most efficient method, highly stable for Q values inside the range where the constant Q linear theory for attenuation is valid. The trace filtered using the downward continuation method has a very good phase correction, less than one time sample for Q greater than 50, but has a poor performance in recovering amplitudes. The last method evaluated is an application of the linear nonstationary filtering theory, by using generalized Fourier integrals, or pseudodifferential operators, to apply the Q filter. This approach is highly stable and the output obtained has better amplitude and resolution recovery. The efficiency of this last method is intermediate between the other two assessed methods.

FUTURE WORK

The main objective of this work is to understand and assess the existent methods for inverse Q filtering in order to take them as reference to evaluate the performance of the Gabor deconvolution method. A necessary future development is the analysis of the influence of factors such as the uncertainty in the estimation of Q, the variation of Q with depth and the presence of noise on the output generated by the filters.

REFERENCES

Aki, K., and Richards, P. G., 2002, *Q*uantitative seismology, theory and methods. University Science Books.

Baraniuk, R. G., and Jones, D. L., 1993, A signal dependent time-frequency representation: optimal kernel design. IEEE Trans. on Signal Processing, **41**, 1589-1602.

Claasen, T., and Mecklenbauer, W., 1980, The Wigner distribution , – a tool for time-frequency signal analysis, Philips Journal of Research, **35**, 217-250.

Cohen, L.,1995, Time Frequency Analysis. Prentice Hall PTR.

Dasgupta, R., and Clark, R. A., 1999, Estimation of Q from seismic surface reflected data: Geophysics, **63**, 2120-2128

Gabor, D., 1946, Theory of communication: J. Inst. Electr. Eng., **93**, 429-457.

Grossman, J. P., Margrave G. F., Lamoureux M. P., and Aggarwala, R., 2002, Constant Q wavelet estimation via a Gabor spectral model : CSEG Convention Expanded Abstracts.

Grossman, J. P., Margrave G. F., and Lamoureux M. P., 2002, Constructing nonuniform Gabor frames from partition of unity. CREWES Research Report, **14**

Kjartansson, E., 1979, Constant Q wave propagation and attenuation: J. Geophysics. Res., 84, 4737-4748.

Hale, D., 1981, An Inverse *Q* filter: SEP report **26**.

Iliescu, V., and Margrave G. F., 2002, Reflectivity amplitude restoration in Gabor deconvolution: CSEG Convention Expanded Abstracts.

Iliescu, V., 2002, Seismic signal enhancement using time-frequency transforms. Thesis (M.Sc.)--University of Calgary,

Margrave, G. F., 1998, Theory of nonstationary linear filtering in the Fourier domain with application to time-variant filtering: Geophysics, 63, 244-259.

Margrave, G. F. and Lamoureux M. P. 2002, Gabor deconvolution: 2002 CSEG Annual Convention, Calgary, AB.

Margrave G. F., Dong, L. Gibson, P., Grossman, J. P., Henley D., and Lamoureux M. P., 2003, Gabor Deconvolution: Extending Wiener's Method to nonstationarity. CREWES Research Report, **15**.

Montana, Carlos A. and Margrave, Gary F., 2004, Phase correction in Gabor deconvolution: CREWES Research Report, **16**.

Mertins, A., 1999, Signal Analysis: John Wiley and Sons.

Ozaaktas, H. M., Zalevsky Z. and Kutay, M. A., 200, The fractional Fourier transform with applications in Optics and Signal processing. John Wiley and Sons.

Peacock, K. L., and Treitel, S., 1969, Predictive deconvolution: Theory and practice: Geophysics, **34**, 155-169.

Robinson E. A. and Treitel, S. 1967, Principles of digital Wiener filtering: Geophys. Prosp., **15**, 311-333.

Saggaf, M.M., and Robinson, E. A., 2000, A unified framework for the deconvolution of traces of nonwhite reflectivity: Geophysics, **65**, 1660-1676.

Schoepp, A. R., and Margrave, G. F., 1998, Improving seismic resolution with nonstationary deconvolution: 68th Annual SEG meeting, New Orleans, La.

Schoepp, A. R., 1998, Improving seismic resolution with nonstationary deconvolution. Thesis (M.Sc.)--University of Calgary

Solano G. and Schmidt D., 2004, VSP study on attenuation in oil sands: CSEG expanded abstracts.

Stacey F. D., Gladwin M. T., McKavanagh, B., Linde A. T. and Hastie, L. M., 1975, Anelastic damping of acoustic and seismic pulses: Geophysical Survey, **2**, 133-157.

Steeghs P. and Drijkoningen G.,,2001, Seismic sequence analysis and attribute extraction using quadratic time-frequency representations: Geophysics, **66**, 1947-1959.

Wang, Y.,2002, An stable and efficient approach of inverse *Q* filtering: Geophysics, **67**, 657-663.

Yilmaz, O., 2000, Seismic Data Processing: Soc. Of Expl. Geophys.

ACKNOWLEDGEMENTS